Quasi-spherical cavity resonators for metrology based on the relative dielectric permittivity of gases

Eric F. May,[a] Laurent Pitre,[b] James B. Mehl,[c] Michael R. Moldover,[d] and James W. Schmidt
Process Measurement Division, National Institute of Standards and Technology, Gaithersburg, Maryland 20899-8360

(Received 20 April 2004; accepted 23 June 2004; published 22 September 2004)

We evaluate a quasi-spherical, copper, microwave cavity resonator for accurately measuring the relative dielectric permittivity $\epsilon_r(p,T)$ of helium and argon. In a simple, crude approximation the cavity's shape is a triaxial ellipsoid with axes of length $a, 1.001a$ and $1.005a$, with $a=5$ cm. The unequal axes of the quasi-sphere separated each of the triply degenerate microwave resonance frequencies of a sphere $(f_{11}^{TM}, f_{12}^{TM}, \ldots, f_{11}^{TE}, f_{12}^{TE}, \ldots)$ into three nonoverlapping, easily measured, frequencies. The frequency splittings are consistent with the cavity's shape, as determined from dimensional measurements. We deduced $\epsilon_r(p,T)$ of helium and of argon at 289 K and up to 7 MPa from the resonance frequencies f_{ln}^{σ}, the resonance half-widths g_{ln}^{σ}, and the compressibility of copper. Simultaneous measurements of $\epsilon_r(p,T)$ with the quasi-spherical resonator and a cross capacitor agreed within 1×10^{-6} for helium, and for argon they differed by an average of only 1.4×10^{-6}. This small difference is within the stated uncertainty of the capacitance measurements. For helium, the resonator results for $\epsilon_r(p,T)$ were reproducible over intervals of days with a standard uncertainty of 0.2×10^{-6}, consistent with a temperature irreproducibility of 5 mK. We demonstrate that several properties of quasi-spherical cavity resonators make them well suited to $\epsilon_r(p,T)$ determinations. Ultimately, a quasi-spherical resonator may improve dielectric constant gas thermometry and realize a proposed pressure standard based on $\epsilon_r(p,T)$. [DOI: 10.1063/1.1791831]

I. INTRODUCTION

We report progress towards the goal of using a microwave cavity resonator to measure the relative dielectric permittivity $\epsilon_r(p,T)$ of helium with an uncertainty on the order of 0.05 ppm. (1 ppm = one part in 10^6) Such accurate measurements as a function of temperature T and pressure p would improve existing determinations of the thermodynamic temperature by dielectric constant gas thermometry (DCGT)[1] and they would realize a proposed primary pressure standard (PPS).[2] Both DCGT and the PPS use the virial expansion of the pressure as a function of the density ρ and temperature

$$p = \rho RT(1 + B\rho + C\rho^2 + \cdots), \tag{1}$$

and the similar virial expansion for the molar polarizability, $\wp$,

$$\wp = \left(\frac{\epsilon_r - 1}{\epsilon_r + 2}\right)\frac{1}{\rho} = A_\epsilon(1 + b\rho + c\rho^2 + \cdots). \tag{2}$$

(Here, B and C are the temperature-dependent density virial coefficients; R is the molar gas constant; b and c are the dielectric virial coefficients; and A_ϵ is the molar polarizability in the limit of zero pressure.) The density is eliminated iteratively[2] from Eqs. (1) and (2) to obtain

$$\left(\frac{\epsilon_r - 1}{\epsilon_r + 2}\right) = \frac{A_\epsilon p}{RT}\frac{(1 + bp/(RT) + \cdots)}{(1 + Bp/(RT) + \cdots)}. \tag{3}$$

For DCGT, one measures $\epsilon_r(p,T)$ on an isotherm, trusts the pressure instrumentation, and uses Eq. (3) to deduce the temperature. For the PPS, one performs the same measurements at the defined temperature of the triple point of water ($T_{tpw} \equiv 273.16$ K, exactly) and uses Eq. (3) to deduce the pressure. The quantity A_ϵ in Eq. (3) has been calculated *ab initio* with an uncertainty of less than 1 ppm for helium.[3] Such accurate calculations cannot be performed for any other gas; thus, helium must be used for the PPS. However, the dielectric permittivity of helium is so small $[\epsilon_r(7\text{ MPa}, 273\text{ K}) \approx 1.005]$ that a measurement of ϵ_r must have a relative uncertainty of 0.05 ppm to calibrate a conventional piston-cylinder pressure gage with an uncertainty of 10 ppm at 7 MPa.

Here, we evaluate a prototype, quasi-spherical, copper microwave cavity resonator for measuring $\epsilon_r(p,T)$ with sub-ppm uncertainties. (See Fig. 1.) In this preliminary work, the uncertainties of the measurements were not intrinsic to the quasi-spherical cavity; they resulted from our limited ability to measure its dimensions, control its temperature and measure the gas pressure. We illustrate these circumstances with two examples: First, we used the cavity resonator to measure

[a]Guest Scientist: American Australian Association Fellow. Electronic mail: eric.may@nist.gov
[b]Guest Scientist: permanent address BNM-INM\CNAM, 292 Rue St. Martin, Paris 75003, France.
[c]36 Zunuqua Trail, PO Box 307, Orcas, Washington 98230-0307, U.S.A.
[d]Author to whom correspondence should be addressed. Electronic mail: michael.moldover@nist.gov

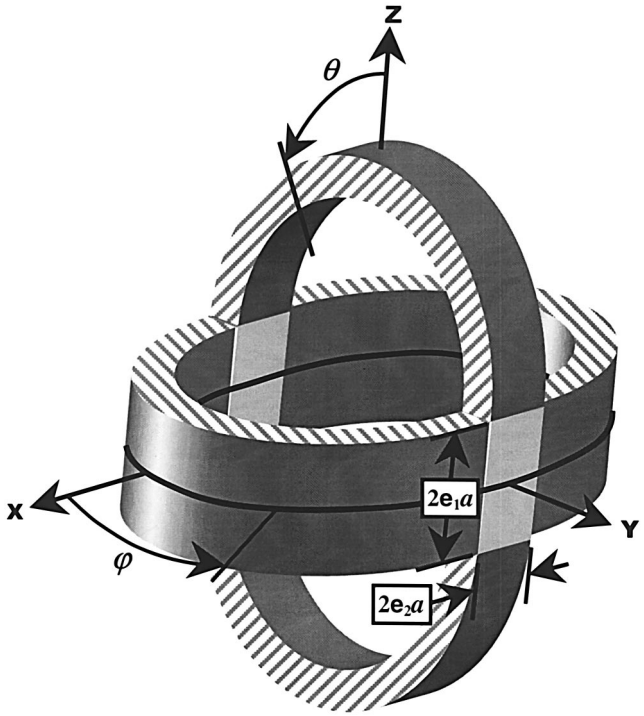

FIG. 1. Cut-away schematic of a quasi-spherical cavity resonator with a "race-track" shape. The narrow, orthogonal cylindrical sections have widths of $e_1 a$ and $e_2 a$, where a is the radius of the spherical sections.

$\epsilon_r(p,T)$ of helium at 289 K at pressures up to 7 MPa. The difference between the cavity values of $\epsilon_r(p,T)$ and those calculated *ab initio* averaged $(0.18 \pm 0.21) \times 10^{-6}$. (The uncertainty presented here and below is one standard deviation.) In this example, the uncertainty is consistent with 5 mK temperature drifts occurring over intervals of days. Second, using the apparatus sketched in Fig. 2, we measured $\epsilon_r(p,T)$ of argon using the cavity resonator and, simultaneously, using a well characterized cross capacitor.[4,5] The comparison of the simultaneous measurements is insensitive to the uncertainties from the temperature, pressure, and impurities in the argon. The average difference between the argon values of $\epsilon_r(p,T)$ measured with the two instruments was 1.4×10^{-6}; this difference probably resulted from small biases in the capacitance measurements. These examples imply that smaller uncertainties will result as we refine the apparatus and develop the ability to compare one cavity resonator to another.

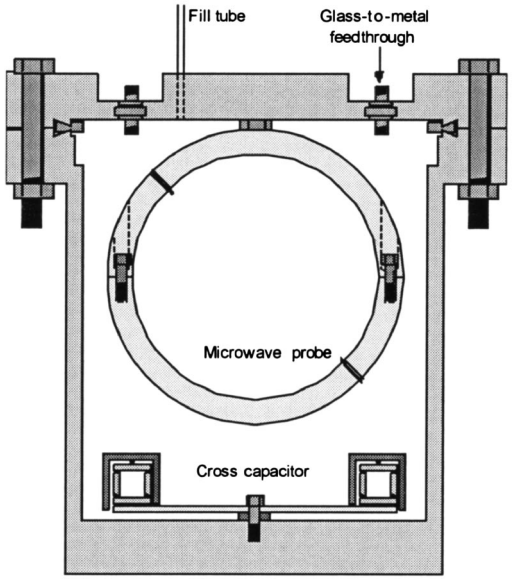

FIG. 2. Cross-section of the pressure vessel containing the quasi-spherical resonator and the cross capacitor from Ref. 4.

The shape of the quasi-spherical cavity resonator was sufficiently close to that of a reference sphere that perturbation theory accurately predicted the resonance frequencies, half-widths, and eigenfunctions of the microwave modes. The intentionally asymmetric shape completely lifts the threefold degeneracy of the eigenfrequencies $(f_{11}^{TM}, f_{12}^{TM}, \ldots, f_{11}^{TE}, f_{12}^{TE}, \ldots)$ of an ideal sphere with equivalent volume, splitting each of them into three nonoverlapping, component frequencies. (In the notation f_{ln}^{σ}, the superscripts TE and TM identify the transverse electric and transverse magnetic modes, respectively, and the subscripts l and n identify the eigenfunction.) Since the components do not overlap, the resonance frequencies of each mode can be determined with relative uncertainties of 10^{-8}, or less.

For completeness, we mention competing techniques for accurately measuring $\epsilon_r(p,T)$. Two of us (M.R.M. and J.W.S.) are actively improving cross capacitors to measure $\epsilon_r(p,T)$ at audio frequencies.[4,5] Stone and Stejskal are improving Fabry–Perot interferometers to measure $\epsilon_r(p,T)$ in gases at optical frequencies.[6] Ewing and Royal[7] used a small (~ 1 cm^3), pressure-compensated, cylindrical cavity to measure $\epsilon_r(p,T)$ of nitrogen with an uncertainty of approximately ± 2 ppm. At this time, it is impossible to predict which, if any, of these technologies will be most useful for DCGT and for a PPS. However, quasi-spherical cavity resonators have several advantages compared with other techniques. First, instrumentation for measuring frequency ratios to better than 0.01 ppm is readily available, whereas capacitance ratios can be measured only to about 1 ppm with commercially available bridges. Second, quasi-spherical cavities have microwave modes that are insensitive to the presence of films such as oxides, oil deposits, or adsorbed water on any surface. Finally, the deformation under hydrostatic pressure of an artifact used to determine accurate values of $\epsilon_r(p,T)$ must be predictable and reproducible, even if it is made of a material that deforms anisotropically. Quasi-spherical cavities have a relatively simple construction and any anisotropic deformation can be quantatively measured because the fractional frequency splittings within a microwave triplet are related to the resonator's dimensions in each direction.

Perhaps quasi-spherical cavity resonators will be applied to other metrological problems. Fellmuth and Fischer propose to measure accurately both the temperature and the pressure and to redetermine the Boltzmann constant $k_B \equiv R/N_A$ using Eq. (3).[8] Tobar *et al.*[9] proposed a new Michelson–Morley-type experiment in which they measure the beat frequency of two nearly degenerate electromagnetic modes propagating orthogonally within a single spheroidal cavity. Their experiment might benefit from the additional splitting of nearly degenerate modes resulting from the lower symmetry of a quasi-spherical cavity.

TABLE I. Properties of the lowest-frequency, triply degenerate modes of a spherical cavity. The estimates assume that the cavity's radius $a=50$ mm and that the conductivity of the copper bounding the cavity is $\sigma=6.04\times10^7$ S m^{-1}. The eigenvalues ξ_{ln}^{σ} are independent of the radius and can be computed numerically with arbitrary precision.

Mode	ξ_{ln}^{σ}	f_{ln}^{σ}/GHz	$10^6\delta$/m	g_{ln}^{σ}/kHz	Q
TM11	2.743 707 2	2.62	1.27	45.3	28 900
TE11	4.493 409 4	4.29	0.99	42.5	50 400
TM12	6.116 764 2	5.84	0.85	52.4	55 600
TE12	7.725 251 8	7.36	0.76	57.7	63 800

II. THEORY FOR A PROTOTYPE QUASI-SPHERICAL CAVITY

A. Prototype "race-track" resonator

In Ref. 10, Mehl *et al.* developed the theory for the prototype quasi-spherical resonator sketched in cut-away form in Fig. 1. Every planar cross-section of the resonator perpendicular to either the *x*- or the *z*-coordinate axes yields a race-track shaped curve; i.e., a closed curve composed of two semicircles separated by two (short) straight line segments. The prototype resonator was composed of two quasi-hemispheres bolted together at their "equator" in the *xy* plane. Although each quasi-hemisphere was a single piece of copper, its shape can be visualized as an assembly of seven parts. Two of these parts are not shown in Fig. 1; each of these is a quarter of a spherical shell with inner radius a; they are separated from each other in the *x*-direction by the third part, a section of a cylinder of thickness $2e_2a$. The remaining four parts are located at the equator of each quasi-hemisphere; they extend the quasi-hemisphere in the *z*-direction a distance e_1a. The extension is composed of two sections of a cylinder separated by two rectangles of width $2e_2a$ and height e_1a. (In Fig. 1, the rectangles have a lighter shading than the other parts.)

We now quote well-known results for spherical cavities and the results for quasi-spherical cavities from Mehl *et al.*[10] that are needed for the present applications.

B. Theory for spherical cavity resonators

In spherical coordinates (r,θ,ϕ), the electric and magnetic fields within an ideal spherical cavity with a perfectly conducting surface may be constructed from the functions (see, for example, Harrington[11])

$$\Phi_{lnm}=j_l(\xi_{ln}^{\sigma}r/a)Y_{lm}(\theta,\phi), \tag{4}$$

where j_l is a spherical Bessel function, Y_{lm} is a spherical harmonic, a is the cavity radius, and ξ_{ln}^{σ} is an eigenvalue, determined by the electromagnetic boundary conditions. The superscript σ distinguishes between TM and TE modes. The eigenvalues for the modes of interest in this experiment are listed in Table I. The eigenfrequencies f_{ln}^{σ} of each mode are

$$f_{ln}^{\sigma}=\frac{c\xi_{ln}^{\sigma}}{2\pi a}=\frac{1}{\sqrt{\mu_0\mu_r\epsilon_0\epsilon_r}}\left(\frac{\xi_{ln}^{\sigma}}{2\pi a}\right). \tag{5}$$

In Eq. (5), c is the speed of the electromagnetic wave in the gas filling the cavity; ϵ_r and μ_r are the relative electric permittivity and magnetic permeability of the gas; $\mu_0\equiv4\pi\times10^{-7}$ N A^{-2} is the magnetic constant; $\epsilon_0\equiv1/(\mu_0c_0^2)$ is the electric constant, and $c_0\equiv299\,792\,458$ m s^{-1} is the defined speed of light in vacuum. For a sphere, the eigenfrequencies are $(2l+1)$-fold degenerate and nontrivial solutions of Maxwell's equations require that $l\geqslant1$; thus, no microwave singlets exist.

In this work, we assume that $\mu_r(p,T)\equiv1$ for both helium and argon. For helium, we estimate the small error in this approximation by using the *ab initio* values for the molar magnetic susceptibility,[12] $4\pi\times(-1.95\pm0.05)\times10^{-6}$ cm^3 mol^{-1}, and the molar electric polarizability[3] $A_\epsilon\approx0.517$ cm^3 mol^{-1} to calculate $[\mu_r(p,T)-1]/[\epsilon_r(p,T)-1]=-1.58\times10^{-5}$. (Conversion of the magnetic susceptibility from CGS to SI units requires a factor of 4π.) We conclude that in future work, the proposed pressure standard cannot neglect μ_r for helium. For argon, we use the experimental values for the molar magnetic susceptibility,[13] $4\pi\times(-19.3\pm0.05)\times10^{-6}$ cm^3 mol^{-1}, and the molar electric polarizability[5] $A_\epsilon=4.142$ cm^3 mol^{-1} to calculate $[\mu_r(p,T)-1]/[\epsilon_r(p,T)-1]=-1.94\times10^{-5}$.

If the boundary surface is an imperfect conductor, the electromagnetic fields within the metal decay exponentially with depth. The decay length is

$$\delta=(\pi\mu_{r,\mathrm{cond}}\mu_0\sigma_{\mathrm{cond}}f)^{-1/2}, \tag{6}$$

where $\mu_{r,\mathrm{cond}}$ and σ_{cond} are the relative magnetic permeability and electrical conductivity of the bounding surface. For copper[14] at 289 K, $\sigma_{\mathrm{cond}}\approx6.04\times10^7$ S m^{-1} and $\mu_{r,\mathrm{cond}}\approx1-9.64\times10^{-6}$. The penetration of the current reduces the resonance frequencies and gives them a finite half-width. For a good conductor such as copper, both effects can be compactly expressed.[15] For TE modes, the effect of finite conductivity is

$$\left(\frac{\Delta f_{\mathrm{cond}}+ig}{f}\right)_{ln}^{TE}=\frac{\delta_{ln}^{TE}}{a}\left(\frac{-1+i}{2}\right), \tag{7a}$$

whereas for TM modes it is

$$\left(\frac{\Delta f_{\mathrm{cond}}+ig}{f}\right)_{ln}^{TM}=\frac{\delta_{ln}^{TM}}{a}\left(\frac{-1+i}{2}\right)\frac{(\xi_{ln}^{TM})^2}{(\xi_{ln}^{TM})^2-l(l+1)}. \tag{7b}$$

For determinations of $\epsilon_r(p,T)$ made with (quasi-)spherical cavities, the conductivity perturbation Δf_{cond} must be added to the frequency given by Eq. (5). Equations (6), (7a), and (7b) were used to calculate the theoretical values of δ and the quality factor $Q\equiv f_{ln}^{\sigma}/(2g_{ln}^{\sigma})$ relevant to this work, and these values are listed in Table I. (Here the superscript σ distinguishes between TM and TE modes and should not be confused with the symbol for conductivity.) Alternatively, the theoretical quality factor can be calculated by determining the surface resistivity and geometric factor of each mode.[16]

Using perturbation theory (see, for example, Harrington[11]), the frequency shift caused by a uniform insulating film of thickness h coating the inside surface of a spherical resonator can be estimated. The film might be an oxide, adsorbed water, pump oil, etc. It can be shown that a film of permeability μ_{film}, and permittivity ϵ_{film} will perturb the frequency of a TE mode by

$$\left(\frac{\Delta f_{\rm film}}{f}\right)_{ln}^{\rm TE} \cong -\left(\frac{\mu_{\rm film}}{\mu_{\rm gas}}-1\right)\left(\frac{h}{a}\right)-\frac{(\xi_{ln}^{\rm TE})^2}{3}\left(\frac{\epsilon_{\rm film}}{\epsilon_{\rm gas}}-1\right)\left(\frac{h}{a}\right)^3. \tag{8}$$

The equivalent perturbation of the TM modes is

$$\left(\frac{\Delta f_{\rm film}}{f}\right)_{ln}^{\rm TM} \cong -\left(\frac{\epsilon_{\rm film}}{\epsilon_{\rm gas}}-1\right)\left(\frac{h}{a}\right)-\frac{(\xi_{ln}^{\rm TM})^2}{3}\left(\frac{\mu_{\rm film}}{\mu_{\rm gas}}-1\right)\left(\frac{h}{a}\right)^3. \tag{9}$$

Thus, ratios such as $\langle f+g\rangle_{11}^{\rm TE}/\langle f+g\rangle_{11}^{\rm TM}$ might detect the presence of a film with high sensitivity. If the film is nonmagnetic, $(h/a)^3$ will probably be so small that $(\Delta f_{\rm film}/f)_{ln}^{\rm TE}$ will be undetectable. The insensitivity of the TE modes to dielectric films is due to the fact that the electric field of these modes at the cavity boundary has no normal component and a vanishingly small tangential component.

A result somewhat analogous to Eq. (8) exists for cross capacitors, but not for simple capacitors such as parallel plates or coaxial cylinders. Shields [17,18] showed that a dielectric film on the four electrodes of a cross capacitor changes the cross capacitance $C_{\rm x}$ by

$$\frac{\Delta C_{x,\rm film}}{C_{\rm x}} \propto \left(\frac{\epsilon_{\rm film}}{\epsilon_{\rm gas}}-1\right)\left(\frac{h}{b}\right)^2, \tag{10}$$

where h is the thickness of the film and b is the distance between the opposite pairs of the electrodes of the cross capacitor. The toroidal cross capacitor used here has $b \approx 10$ mm. Hence, the presence of a surface film on either the cross capacitor or the quasi-spherical resonator used in this work should have a negligible impact on the measured values of $\epsilon_{\rm r}(p,T)$. Furthermore, any differences due to the operating frequency of each instrument are negligibly small for the fluids studied here. Helium's *ab initio* dynamic polarizability increases quadratically with frequency,[6,19] and for helium $[A_\epsilon(10\ {\rm GHz})/A_\epsilon(0\ {\rm GHz})-1]\approx 2.57\times 10^{-12}$. For argon, based on experimental measurements of the refractive index at various wavelengths[20] and assuming a quadratic frequency dependence, we estimate $[A_\epsilon(10\ {\rm GHz})/A_\epsilon(0\ {\rm GHz})-1]\approx 7\times 10^{-12}$.

C. Theory for quasi-spherical cavity resonators

The deviation of a race-track shaped quasi-spherical cavity resonator from an ideal reference sphere is characterized by two geometrical parameters: e_1 and e_2. The shape perturbation separates the $l=1$ triplets into components with axes of rotational symmetry coincident with the x, y, and z axes of the quasi-sphere. The perturbed eigenfrequencies are[10]

$$\left(\frac{\Delta f_{\rm shape}}{f}\right)_{1np}^{\sigma} = \left(\frac{1}{8}\right) D_{1n}^{\sigma} \begin{cases} (-e_1+2e_2) & (p=x) \\ (-e_1-e_2) & (p=y) \\ (2e_1-e_2) & (p=z) \end{cases}, \tag{11}$$

with

$$D_{1n}^{\rm TE}=\left(\frac{1}{2}\right) \quad \text{and} \quad D_{1n}^{TM}=\left(\frac{1}{2}+\frac{3}{(\xi_{1n}^{\rm TM})^2-2}\right). \tag{12}$$

We have introduced the additional subscript p to distinguish between the three components: the mode with $p=z$ corresponds to the mode with $m=0$ in Eq. (4), while the x- and y-modes are linear combinations of the $m=\pm 1$ modes. In Eq. (11), we also use the definition $\Delta f_{\rm shape} \equiv f(e_1,e_2)-f_{1n}^{\sigma}$ for the difference between the shape-perturbed eigenfrequencies and the unperturbed eigenfrequencies of an ideal reference sphere. The latter are given by Eq. (5), where the radius a in Eq. (5) is chosen so that the reference sphere and the quasi-sphere have equal volumes. Inspection of Eq. (11) shows that the average value of $\Delta f_{\rm shape}$ is zero, when the average is taken over the three components ($p=x,y$, and z). This is a specific example of the general result (to first order in e_1 and e_2) proven in Mehl and Moldover.[21]

Thus, by modification of Eq. (5) to account for the frequency perturbations due to boundary conductivity and shape, a radius (for the equivalent reference sphere) a_{ln}^{σ} can be determined from each microwave triplet.

$$a_{ln}^{\sigma}=\frac{c_0}{2\pi\sqrt{\mu_r\epsilon_r}}\frac{\xi_{ln}^{\sigma}}{\langle f+g\rangle_{ln}^{\sigma}}. \tag{13}$$

Here the angled brackets denote an average over all triplet components. Alternatively, by measuring isothermal frequency *ratios* and accounting for pressure-induced changes in radius, the fluid's dielectric permittivity can be determined

$$\epsilon_r=\frac{1}{\mu_r}\left(\frac{\langle f+g\rangle_{ln,0}^{\sigma}}{\langle f+g\rangle_{ln}^{\sigma}(1-(k_T/3)p)}\right)^2. \tag{14}$$

In Eq. (14), the subscript "0" denotes the average triplet frequency under vacuum, and $k_{\rm T}$ is the effective isothermal compressibility of the cavity. The accuracy with which this average can be measured is determined by how well each individual component can be resolved.

The components of any microwave triplet will be well separated if the fractional frequency splitting is at least a small multiple of Q^{-1}. With $e_2=0.001$ and $e_1=0.002$, the components of the TE11 triplet are fractionally separated by approximately $5/Q$ for a copper resonator with a radius of 50 mm. For all other microwave triplets, the separation is an even larger multiple of Q^{-1}. Mehl *et al.*[10] show that each component of the triplet can be excited with approximately equal amplitude by placing microwave probes near the cavity boundary at $\theta=(\pi/4$ or $3\pi/4)$ and $\phi=(\pi/4, 3\pi/4, 5\pi/4,$ or $7\pi/4)$.

We have not calculated the effect of the shape perturbation on the half-widths of the components. The half-widths are sensitive to the surface-to-volume ratio of the cavity because electromagnetic energy is stored throughout the volume of the cavity while it is dissipated by the currents that flow within the conducting surface bounding the cavity. The surface-to-volume ratio of the quasi-sphere does not have a linear dependence on e_1 or e_2, provided the volume is kept constant. Thus, we expect the half-widths of the quasi-sphere to exceed those of an equal-volume reference sphere by terms on the order of e_1^2, which are too small to detect.

III. APPARATUS

A. Quasi-spheres

Three nearly identical quasi-spherical resonators were machined in the same way; one was made of the aluminum alloy 6061-T6 and two were cut out of the same billet of

oxygen-free high-conductivity (OFHC) copper. One of the copper resonators was drilled to accept acoustic transducers and is now being used for acoustic thermometry.[10] The second copper resonator was used for this work.

Our design specified that each quasi-hemisphere have a spherical section of radius $a=50.00$ mm, cylindrical extensions of lengths $2ae_2=0.1$ mm and $ae_1=0.1$ mm, and a shell thickness of 10.0 mm. The resonator had 3.1 mm diameter holes for electromagnetic probes at $(\theta,\phi)=(\pi/4,\pi/4)$ and $(3\pi/4,3\pi/4)$. A 1.6 mm diameter hole through the shell at $(\theta,\phi)=(\pi/4,5\pi/4)$ allowed gas within the cavity to communicate with gas in the pressure vessel housing the resonator.

The quasi-hemispheres were cut out of the OFHC copper billet using a "five-axis" (three translational plus two rotational axes), numerically programmed, high-speed machining center. This programmable milling machine can fabricate shapes comprised of combinations of spherical and cylindrical sections, with a claimed tolerance of ±0.01 mm. The tolerance is the resolution of a position measurement system, which controls the location of the cutting tool.

Much simpler tools can manufacture an excellent approximation of the race-track quasi-hemisphere. A lathe fitted with a pivoting tool holder and a four-jawed chuck is sufficient. One begins with a cylindrical billet held in the chuck. The pivoting tool is used to cut both a hemispherical cavity and the cylindrical extension of width e_1a at the hemisphere's equator. Then, two opposing jaws of the chuck are adjusted to translate the axis of the billet parallel to itself a distance $2e_2a$. Finally, the hemispherical and cylindrical cuts are repeated.

Each quasi-hemispherical shell was terminated at the equator by a flat surface shaped like a race-track. Three holes with diameters of 3 mm were drilled into this surface to accommodate locating pins. Each shell contained six holes to accommodate 4–40 bolts. For the "southern hemisphere" the bolt holes were tapped; for the "northern hemisphere" they were clear and counter-sunk. When the resonator was assembled, the bolts were firmly tightened with care taken not to damage the copper threads. As the bolts were tightened, the *Qs* of the microwave resonances increased. This observation led us to lap the equatorial surfaces with a 1 micrometer grit and then to thoroughly clean these surfaces.

B. Instruments and gases

Figure 2 shows a cross-section of the pressure vessel containing the quasi-spherical cavity resonator and a cross capacitor that had been characterized in our laboratory.[4] This arrangement facilitated the comparison of the resonator to the cross capacitor with confidence that both instruments were immersed in the identical gas at nearly identical temperatures and pressures. These comparisons were made without the benefit of an apparatus that could maintain the purity of the gases and without using a pressure balance, a high-performance thermostat, or a thermometer inside the pressure vessel.

The resonator was hung from the lid of the pressure vessel by a 1/4–20 threaded copper rod that fit into blind, threaded holes in the resonator and in the lid. The cross capacitor was bolted to the base of the pressure vessel, but separated from the base by a washer. The approximately single-point supports for the resonator and the capacitor prevented the pressure-induced flexing of the pressure vessel from deforming these precise instruments. The stainless-steel pressure vessel was sealed by compressing a copper gasket between knife edges, as is commonly done in high vacuum apparatus. The all-metal seal was successful up to 7 MPa; it did not contain polymers that might contaminate the test gases.

The pressure vessel was immersed in a stirred oil bath that had a homogeneity and short-term stability (several weeks) better than 0.01 K. Coaxial glass-to-metal feedthroughs passed through the lid of the pressure vessel. Coaxial cables led from the lid through the oil bath to the microwave vector analyzer and the capacitance bridge. Gas was admitted to the pressure vessel by a 1.8 mm inside diameter tube. The tube led from the pressure vessel through the bath to a pressure gauge and an isolation valve. The unthermostatted volume in the tube, pressure gauge and valve was 1.8 cm^3. This is small compared with the 2100 cm^3 volume of the pressure vessel; however, it is still too large for the proposed applications.

The pressure was measured using a quartz crystal pressure gauge with a full scale of 21 MPa and an estimated uncertainty of ±0.3 kPa over the range 0–7 MPa. Under steady state conditions, the temperature of the bath, the pressure vessel, and the resonator were all assumed to be equal. We did not install a standard platinum resistance thermometer in the pressure vessel because we feared subjecting its delicate glass-to-metal seals to pressures of 7 MPa. The bath temperature was measured with an estimated uncertainty of ±0.02 K using a commercially manufactured resistance thermometer and platinum sensor. The resonance frequencies were determined from transmission measurements using vector network analyzers, phase locked to a 10 MHz reference oscillator. Most of the data were taken below 6 GHz using an older analyzer. Our most precise frequency measurements were made using another analyzer that operated up to 8.5 GHz. Unfortunately, the capacitance bridge that we previously used with the cross capacitor was not available. The commercially manufactured bridge that we did use had a looser specification (5 ppm vs 3 ppm). This might explain why the present capacitance results are slightly less consistent than those previously reported; however, the capacitance results are consistent with the specifications supplied by the bridge's manufacturer.

The supplier of the helium stated its purity was 99.9999%, by volume, and that it had a water content of less than 0.2 ppm. The supplier of the argon stated that its purity was 99.9995% by volume. The dominant impurity was nitrogen, which has a molar polarizability only 6% greater than that of argon. The supplier stated that the water content of the argon was less than 0.02 ppm, by volume.

C. Heat transfer and temperature control

Considerations of heat transfer significantly constrain the design and operation of the quasi-spherical resonator. The data were taken in order of increasing pressure from 100 kPa

to 7 MPa in 1 MPa steps, and then in decreasing steps of 1 MPa. When gas is pumped into the pressure vessel the gas temperature rises, which in turn heats the resonator, the cross capacitor, and the pressure vessel. The pressure vessel and most of the gas within it cool back to the bath's temperature within tens of seconds. However, the resonator, the cross capacitor, and the gas within them return to the bath temperature slowly. The resonator cooled most slowly with a time constant of one hour. Thus, we allowed at least 8 hours for equilibration following each pressure change before making frequency and capacitance measurements. Unfortunately, the apparatus was not completely automated and, consequently, a run of 15 measurements along an isotherm took up to 8 days. Obviously, a stronger thermal link would speed up the measurements; however, such a link must be designed so that it does not transmit stress to the resonator. Alternatively, a smaller resonator might be used. (The present size of the resonator was set by a requirement of acoustic thermometry; namely, that its volume be large compared with the effective volume of the acoustic transducers.)

The contemplated pressure standard requires accurate temperature control for two reasons. First, Eq. (3) implies that the uncertainty of the temperature of the gas must be less, fractionally, than the uncertainty of the pressure. For example, a fractional pressure uncertainty of 10 ppm requires that the temperature uncertainty be less than 2.7 mK at 273.16 K. Second, Eq. (14) implies that $\epsilon_r(p,T)$ is determined from the *square* of isothermal frequency ratios and, thus, the fractional uncertainty of the resonator's thermal expansion must be less than half the desired uncertainty of ϵ_r. For example, a fractional uncertainty of 0.05 ppm in ϵ_r requires an uncertainty of 0.025 ppm in the average radius of the resonator. For a copper cavity of radius 5 cm, this requires a temperature uncertainty of 1.7 mK or less. This second constraint on the temperature control can be relaxed by constructing the resonator from a material with a smaller coefficient of thermal expansion.

IV. MICROWAVE MEASUREMENTS

The TM and TE microwave modes were excited and detected by antennae that were extensions of the center conductors of the coaxial cables. Each center conductor (0.5 mm diameter) was bent into a single loop (2 mm diameter) that nearly touched the outer conductor of the coaxial cable. Loop probes are reactive and can, therefore, load the cavity's resonant frequency;[22] to limit any such effect the coupling of these probes was minimized. Initially, the angular orientations of the loop probes were adjusted so that, for each TE triplet monitored, the three components were excited with approximately equal magnitude. With their angular orientation fixed, the probes were then withdrawn slowly from the resonator while monitoring g_{11}^{TM} (the half-widths of the TM11 components) until g_{11}^{TM} stopped decreasing. This procedure ensured that the loading of all the modes by either the probes or the external circuit was too small to detect.

The coupling of the single-turn loop antennae to the TE11 components was substantially weaker than the coupling to any other components. Consequently, the signal-to-noise ratio for the TE11 components was lower, limiting the precision of the measurements of f_{11}^{TE} and g_{11}^{TE}. After we obtained the results reported here, we learned how to solve this problem using multi-turn antennae.

To determine the frequencies and half-widths of each triplet, the network analyzer was set to sweep through 201 frequencies, spanning approximately 10 MHz and centered approximately at the average triplet frequency. (See Fig. 3.) The analyzer returned values of the complex voltage scattering parameter S_{21}. These data were fitted by the function

$$\boldsymbol{S}_{21}(f) = \sum_p \frac{\boldsymbol{A}_p f}{f^2 - (\boldsymbol{F}_{1np}^{\sigma})^2} + \boldsymbol{B} + \boldsymbol{C}(f - f_*) + \boldsymbol{D}(f - f_*)^2. \tag{15}$$

The fitting parameters were the six complex constants $\mathbf{A}_p, \boldsymbol{B}, \boldsymbol{C}$, and $\boldsymbol{D}$ and the three complex resonance frequencies $\boldsymbol{F}_{1np}^{\sigma} = f_{1np}^{\sigma} + i g_{1np}^{\sigma}$, one for each component of the triplet. In Eq. (15), f is the source frequency and f_* is an arbitrary constant; we choose $f_* = f_{1nx}^{\sigma}$ to avoid numerical problems in the fitting program. The parameters $\boldsymbol{B}, \boldsymbol{C}$, and $\boldsymbol{D}$ account for possible crosstalk and for the effects of the "tails" of the modes other than the triplet under study. For the higher-frequency modes, the quadratic parameters $\boldsymbol{D}$ were statistically significant. In previous work,[23] $\boldsymbol{D}$ was not required because the data typically spanned only a few megahertz; the smaller span was appropriate for the nearly degenerate triplets of a nearly spherical cavity. Figure 3 displays the TM11 triplet and the residuals from a fit. The values of the parameters and their uncertainties are listed in Table II.

The measured half-widths of the resonance frequencies $g_{ln,\mathrm{meas}}^{\sigma}$, exceeded the half-widths $g_{ln,\mathrm{calc}}^{\sigma}$ calculated from the conductivity of copper by $\Delta g_{ln}^{\sigma} \equiv (g_{ln,\mathrm{meas}}^{\sigma} - g_{ln,\mathrm{calc}}^{\sigma}) = (0.1 \text{ to } 2.2) \times 10^{-6} f_{ln}^{\sigma}$, depending upon the mode; values of Δg_{ln}^{σ} at 290 K are listed in Table III. The uncertainty in the literature value for copper's conductivity[14] dominates the uncertainty in Δg_{ln}^{σ}, which is on average $0.3 \times 10^{-6} f_{ln}^{\sigma}$. The value of $g_{ln,\mathrm{meas}}^{\sigma}$, is sensitive to the resonator's surface finish and to the details of a particular mode's surface current distribution. The highest frequency mode ($p=z$) of both the TM triplets had the largest excess half-width because the surface currents for these modes flow along the quasi-sphere's lines of longitude and, therefore, all the current must cross the equatorial break separating the two hemispheres. It is known that these modes are sensitive to the degree of contact between the two hemispheres, and that bolt tightness affects the measured Q.[16] However, we also found that removal of the oxide layer and any surface imperfections on the equatorial seams (by lapping, for example) was crucial for achieving minimal Δg_{ln}^{σ} values.

We do not fully understand why $\Delta g_{ln}^{\sigma} > 0$. However, after accounting for changes in penetration depth, we found that the pressure dependence of Δg_{ln}^{σ} was too small to detect in all of the experiments described below. Since $\epsilon_r(p,T)$ is deduced from the pressure dependence of $\langle f+g \rangle_{ln}^{\sigma}$, our imperfect understanding of Δg_{ln}^{σ} made a negligible contribution to the uncertainty of $\epsilon_r(p,T)$.

From Fig. 3 it is obvious that the separation of the TM11 components is unequal and therefore inconsistent with the

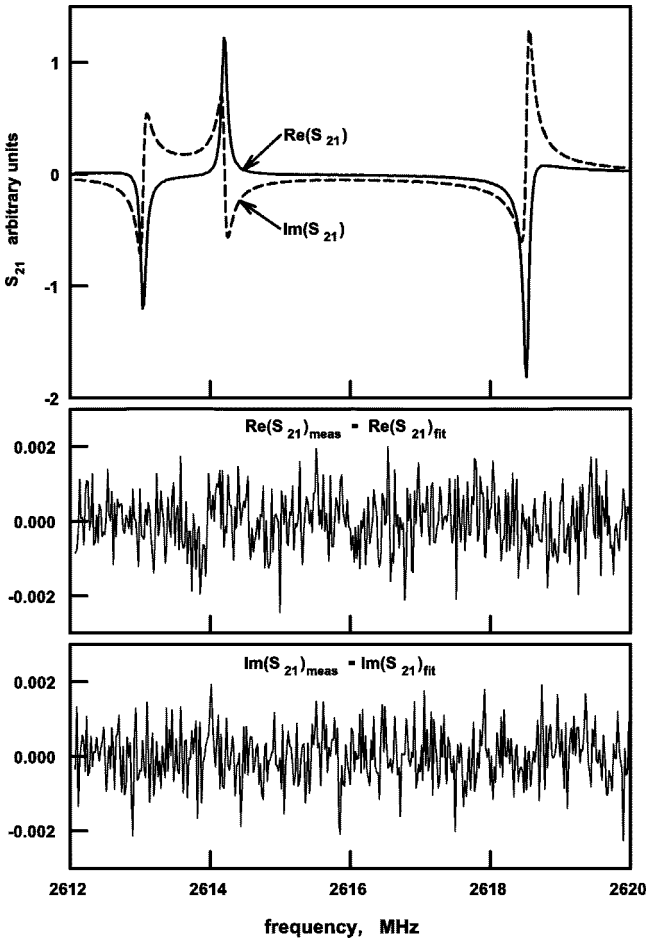

FIG. 3. Complex spectrum in the vicinity of the TM11 triplet and deviations from a fit using Eq. (15). The three components of the triplet are well separated. In this case, the average frequency of the triplet could be determined with a fractional uncertainty of 1.5×10^{-8}.

design values $e_1=0.002$ and $e_2=0.001$. The measured splittings are listed in Table IV together with the values of e_1 and e_2 calculated from the measured splittings by inverting Eq. (11). The average values calculated from the splittings are $(e_1,e_2)=(5.32\pm0.04.\ 1.18\pm0.02)\times10^{-3}$. Thus the microwave data are consistent with the design value of e_2 but inconsistent with the design value of e_1. This inconsistency is of little importance for the proposed applications; however, we were led to make extensive dimensional measurements on the chance that the theory had overlooked some important idea. Instead of flaws in the theory, we found flaws in the fabrication technique.

V. COORDINATE METROLOGY

At our request, the Precision Engineering Division of NIST measured the internal surfaces of the quasi-hemispheres using a coordinate measurement machine (CMM). The CMM had a resolution of 1×10^{-5} mm, a repeatability of 1×10^{-4} mm and an uncertainty of $\pm5\times10^{-4}$ mm or better, depending on the properties of the surface under study. For each hemisphere an origin was established in the equatorial plane, centered approximately in line with the hemisphere's pole. The hemispheres were oriented such that the coordinate axes were consistent with the axes shown in Fig. 1; that is, the cylindrical extension of thickness $2ae_2$ was aligned with the x-axis of the CMM. The coordinate measurements comprised of eight "slices," each separated by a rotation of $\pi/8$ about the z-axis.

Along each slice the coordinates (w,z) were measured over the range $w=(-60,+60)$ mm, where $w=r\sin(\theta)\times\mathrm{Sign}[\sin(\phi)]$ is a generalized axis in the xy plane, which accounts for the rotation of each slice relative to the x-axis. The first and last 10 mm of each slice sampled the planar regions that comprise the equatorial seams and, consistent with the lapping process that each hemisphere was subjected to, the planar regions were found to have sub-micrometer smoothness. The density of the remaining coordinates was not uniform, with the highest density (40 points per mm) occurring in the regions near the cylindrical extensions. The coordinates in the range $w=(-50,+50)$ mm measured for one of the hemispheres are shown in Fig. 4(a).

The sets of coordinates for the cavity's two hemispheres were simply combined, even though they were measured relative to different origins. However, it was found that the two origins were aligned to within a few micrometers. The measured radial coordinates of the resonator's internal surface were regressed to the following expansion of spherical harmonics

$$r=a_{\mathrm{ave}}\left[1-\sum_{l=1}^{\infty}\sum_{m=-l}^{l}c_{lm}Y_{lm}(\theta,\phi)\right]. \tag{16}$$

Here, r is the resonator surface, a_{ave} is the radius of a sphere with equal volume, and the c_{lm} are the spherical harmonic amplitudes that, for $l\geqslant1$, characterize the deviation from a perfect sphere. The regression was conducted using an iterative procedure that determined only those terms that could be justified statistically (95% confidence level). The standard error of the best fit was 0.0051 mm for an expansion with $l\leqslant10$; for this fit only 18 out of a possible 120 terms were statistically significant.

In Fig. 4(b), the designed and fabricated surfaces of the quasi-spherical resonator are shown and in both cases the deviations from an ideal sphere $(c_{lm}Y_{lm}, l\geqslant1)$ have been multiplied by a factor of 100. Instead of a race-track shape, the fabricated cavity had a shape similar to that of a "peanut shell:" It was too narrow at the equator, too large at the poles and the spherical regions were cut too deep. Subsequently, in consultation with the machine shop, we determined that at least part of the deviation of the machined hemispheres from the designed hemispheres was caused by inadequate thermal control of the spindle holding the cutting tool. As the cutting progressed, the spindle warmed and cut deeper hemispheres than we specified. This problem was specific to the particular milling machine used, and has now been rectified.

Mehl *et al.*[10] show that the frequency splittings within the microwave triplets are determined by the values of c_{2m} in Eq. (16). (Misalignment of the hemispheres primarily alters the c_{1m} amplitudes which, to first-order, have no effect on the cavity's eigenfrequencies.) The values of the c_{2m} amplitudes, as determined from the regression to the coordinate data, were used to calculate expected frequency splittings for each triplet and the results are listed in Table V. The frequency

TABLE II. Typical parameter values and uncertainties determined by fitting Eq. (15) to measurements of the TM11 triplet.

Parameter	Re(Parameter)	Im(Parameter)	Uncertainty
$F^{TM}_{1,1,y}$/MHz	2613.042 95	0.046 59	0.000 04
$F^{TM}_{1,1,x}$/MHz	2614.206 00	0.046 64	0.000 04
$F^{TM}_{1,1,z}$/MHz	2618.525 89	0.050 98	0.000 03
A_y	1.1411	0.2173	0.0008
A_x	−1.1777	−0.0805	0.0008
A_z	1.7949	−0.7191	0.0008
B	0.0934	−0.0129	0.0011
C	0.0005	−0.0041	0.0007
D	−0.0001	−0.0002	0.0002

splittings and perturbation parameters, $(e_1, e_2) = (5.44, 1.21) \times 10^{-3}$, determined from the coordinate measurements are in excellent agreement with the measured microwave values listed in Table IV. Thus, in addition to helping identify a fabrication error, the coordinate metrology provided an independent verification of the theory used to describe the microwave and acoustic spectra of quasi-spherical cavity resonators.

VI. CAVITY RADIUS AS A FUNCTION OF FREQUENCY AND PRESSURE

In this section, we compare the average radius of the quasi-spherical cavity determined from the CMM data with the radii determined from four microwave triplets. There is reasonable agreement; the agreement might be improved by analyzing the microwave data with an improved theory that accounts for terms of order e_1^2 and e_2^2.

The regression of Eq. (16) to the measured coordinates leads directly to a value for the radius of a sphere with equivalent volume: at 293.2 K, $a_{ave} = 50.056$ mm. It is difficult to assign an uncertainty to this radius; the uncertainty has contributions from the underlying CMM data and our assumption that the reference sphere's volume was the sum of the volumes of the two quasi-hemispheres. The claimed uncertainty of the CMM data is $\pm 5 \times 10^{-4}$ mm which is 10 ppm of the radius. If the assembled quasi-hemispheres had a gap of 0.5 μm at the equator, the volume of the assembly would exceed that computed from perfect data by 7.5 ppm; this is equivalent to a fractional error of 2.5 ppm in the radius.

Using Eq. (13), we computed the radii a^{σ}_{ln} at 288.94 K from measurements of the microwave triplets when the cavity was evacuated and when it was filled with helium at pressures up to 7 MPa. We approximated μ_r by unity and we determined $\epsilon_r(p,T)$ for helium from Eq. (3) using the *ab initio* values for the parameters $A_\epsilon, b(T)$, and $B(T)$ and experimental values for the higher order terms. All of the helium parameter values came from the same sources used by Moldover and Buckley.[4] Figure 5 displays the equivalent radius as a function of the applied helium pressure at 288.94 K for four triplets. The frequency dispersion of the microwave radii is apparent; at each pressure the four radii have a fractional standard deviation of 16 ppm. The microwave radii measured under vacuum were regressed to the empirical expression

$$a = a_0 + a_1(\langle f + g \rangle^{\sigma}_{ln,0})^2. \tag{17}$$

The extrapolation leads to $a_0 = 50.0572$ mm, which is the most accurate estimate of the cavity radius that can be ob-

TABLE III. Fractional excess half-widths, $10^6(\Delta g^{\sigma}_{ln}/f^{\sigma}_{ln})$, for each mode, p, within the TM11, TE11, TM12, and TE12 triplets at 290 K. The electrical conductivity of copper was estimated to be 6.04×10^7 S m^{-1} using Ref. 14. The uncertainty in $(\Delta g^{\sigma}_{ln}/f^{\sigma}_{ln})$ is approximately ±0.5 ppm for the TM11 triplet and decreases to ±0.2 ppm for the TE12 triplet.

Triplet	$p=y$	$p=x$	$p=z$	Average
TM11	0.6	0.6	2.2	1.1
TE11	1.0	0.8	0.3	0.7
TM12	0.4	0.4	1.4	0.7
TE12	0.5	0.6	0.1	0.4

TABLE IV. Measured fractional frequency splittings, $10^4(\Delta f_{shape}/f)^{\sigma}_{lnp}$ for the triplets TM11, TE11, TM12, and TE12, and the corresponding values of e_1 and e_2 calculated using Eq. (11). An equivalent radius a^{σ}_{ln} determined using Eq. (13), is also listed for each triplet. These measurements were made under vacuum at 290 K.

	TM11	TE11	TM12	TE12
$p=y$	−8.48	−4.07	−4.75	−4.06
$p=x$	−4.03	−1.88	−2.16	−1.76
$p=z$	12.5	5.95	6.91	5.81
$10^3 e_1$	5.37	5.35	5.32	5.26
$10^3 e_2$	1.14	1.17	1.18	1.23
a^{σ}_{ln}[mm]	50.0570	50.0564	50.0558	50.0551

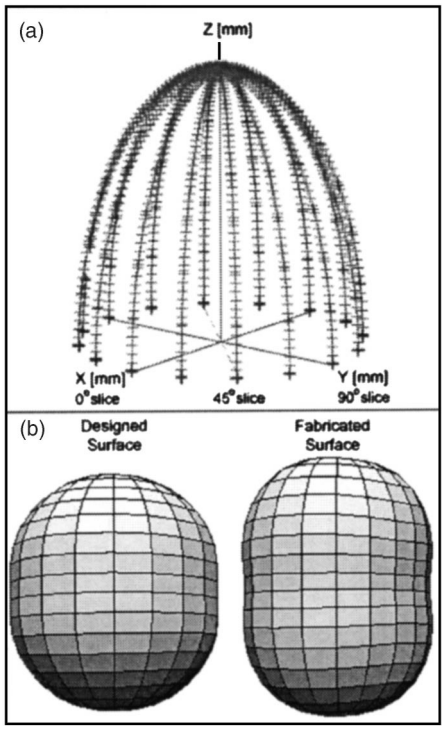

FIG. 4. Results of measurements made with the NIST coordinate measuring machine. (a) Coordinates measured for one of the hemispheres. (b) The designed (left) and fabricated (right) surfaces of the resonator; the deviations of each shape from a perfect sphere have been multiplied by a factor of 100.

TABLE V. Equivalent fractional frequency splittings $10^4(\Delta f_{\text{shape}}/f)^{\sigma}_{lnm}$ for the triples TM11, TE11, TM12, and TE12 determined from a regression of the coordinate measurements to the expansion of spherical harmonics in Eq. (16).

	TM11	TE11	TM12	TE12
$p=y$	−8.68	−4.16	−4.59	−4.16
$p=x$	−3.93	−1.89	−2.08	−1.89
$p=z$	12.6	6.04	6.67	6.04

tained from microwave measurements. Equation (17) reflects our conjecture that the frequency dependence is quadratic (with no linear term) because such a functional form is appropriate for the radially symmetric *acoustic* modes in an ellipsoidal cavity.[24] In principle, the frequency dependence of a^{σ}_{ln} can be accurately computed from perturbation theory and the measured shape of the quasi-spherical cavity. When this is done, we expect the uncertainty of a_0 will approach the precision of the quadratic fit, which is currently 1.8 ppm. If the quasi-spherical cavity had been constructed as designed, ($e_1 \approx 0.002$ instead of $e_1 \approx 0.005$), the dispersion of a^{σ}_{ln} would have been approximately $1/6$ as large. When converted to 293.2 K and 0.1 MPa, the extrapolated microwave value a_0 exceeds the CMM value of a_{ave} by 75 ppm (3.7 μm).

As indicated in Eq. (14), we expect the value of a^{σ}_{ln} to decrease linearly with the applied hydrostatic pressure, with a slope determined by the isothermal compressibility of the copper shell. From the slopes in Fig. 5, we find $k_T = (7.52 \pm 0.02) \times 10^{-12}$ Pa^{-1} at 288.94 K, where the uncertainty is the standard deviation over the four microwave triplets. This value agrees fortuitously well with the value $k_T = (7.52 \pm 0.11) \times 10^{-12}$ Pa^{-1} that we computed from tabulated values of the adiabatic bulk modulus, heat capacity and thermal expansion coefficient of OFHC copper at 295 K.[14] A primary pressure standard would require an independent determination of k_T, with an uncertainty an order of magnitude smaller than that of the present literature value.

VII. PERMITTIVITY MEASUREMENTS

The literature value of k_T and Eq. (14) were used to determine $\epsilon_r(p,T)$ for helium and argon from measurements of the microwave triplets at 288.94 K and pressures to 7 MPa. Here we report three key measures of the resonator's performance. (1) The results for $\epsilon_r(p,T)$ are independent of the triplet used at levels from (1 to 5) $\times 10^{-8}$. (2) The results for $\epsilon_r(p,T)$ of helium are in good agreement with the *ab initio* values: $\Delta\epsilon_r \equiv (\epsilon_{r,\text{resonator}} - \epsilon_{r,\text{ab initio}})$, when averaged over three runs ranges from (0.41 to $-0.05) \times 10^{-6}$, where the uncertainty depends on the uncertainty of the literature value of k_T. (3) The results $\epsilon_r(p,T)$ of helium and argon agree with those determined simultaneously with a cross capacitor within the uncertainty of the capacitance measurements which were on the order of 10^{-6}.

Ratio tests provide the best display of the cavity resonator's potential. We consider the ratio $\langle f+g\rangle^{\text{TM}}_{12}/\langle f+g\rangle^{\text{TM}}_{11} \approx 2.2294$. Figure 6 shows that this ratio did not vary from its average value (with a standard deviation of 1.1×10^{-8})

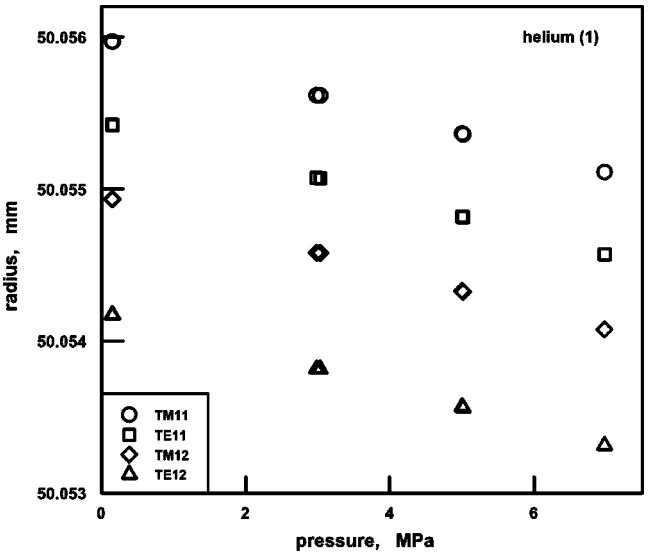

FIG. 5. Variation of the resonator's effective radius as a function of pressure at 288.94 K, inferred from measurements of the microwave triplets and the literature value of $\epsilon_r(p,T)$ for helium.

while the gas pressure was varied from 0 to 7 MPa and back to 0 MPa in three successive runs, two with helium and one with argon. During the helium measurements, $1 < \epsilon_r < 1.0044$; during the argon measurements, $1 < \epsilon_r < 1.0382$. This result combined with Eq. (14) shows that the values of $\epsilon_r(p,T)$ at 2.6 GHz are indistinguishable from the values at 5.8 GHz, as expected. Also, the ratio $\langle f+g\rangle^{\text{TE}}_{11}/\langle f+g\rangle^{\text{TM}}_{11} \approx 1.6377$ was independent of the gas pressure with the larger standard deviation of 5.6×10^{-8}. (The larger standard deviation resulted from the poorer signal-to-noise ratio for the TE11 measurements.) At the level of 5.6×10^{-8}, we are confident that the $\epsilon_r(p,T)$ results are insensitive to the possible presence of thin surface films. Recalling that the $\epsilon_r(p,T)$ results are independent of the triplet used, we plot the remaining results for the TM11 triplet only.

In Fig. 7, the $\epsilon_r(p,T)$ results for three helium runs are compared with the *ab initio* values determined using Eq. (3). The first measurement of each run was used to determine the constant $\langle f+g\rangle^{\sigma}_{ln,0}$ required by Eq. (14). [For run (1) this was done near 0 MPa; for runs (2) and (3) this was done near 0.1 MPa with an appropriate correction.] With this choice, we compute the average of $\Delta\epsilon_r \equiv (\epsilon_{r,\text{resonator}} - \epsilon_{r,ab\ initio})$ over the three runs. We find $\langle \Delta\epsilon_r \rangle = (0.18 \pm 0.21) \times 10^{-6}$. If the literature value of k_T is varied within its published uncertainty, $\langle \Delta\epsilon_r \rangle$ ranges from (0.41 to $-0.05) \times 10^{-6}$. Thus, the most important uncertainty of $\epsilon_{r,\text{resonator}}$ results from the uncertainty of k_T, not from the internal consistency of the resonator measurements.

Given the experimental arrangement shown in Fig. 2, direct comparison of $\epsilon_r(p,T)$ values determined simultaneously with the resonator and the cross capacitor eliminates uncertainties associated with the temperature, pressure, or gas composition. Measurements of the cross capacitance C_x give values of $\epsilon_r(p,T)$ through the relation

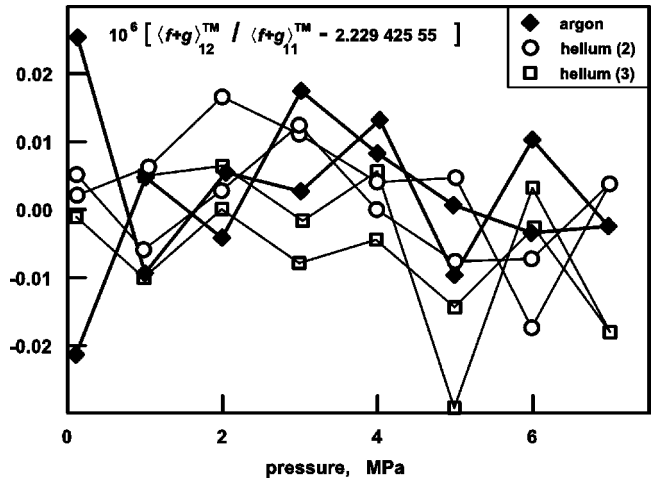

FIG. 6. Consistency of $\epsilon_r(p,T)$ values determined with two different microwave triplets, separated in frequency by a factor of 2.2294. The frequency ratio $\langle f+g\rangle_{12}^{TM}/\langle f+g\rangle_{11}^{TM}$ has a standard deviation of 1.1×10^{-8} for data measured along one argon and two helium isotherms.

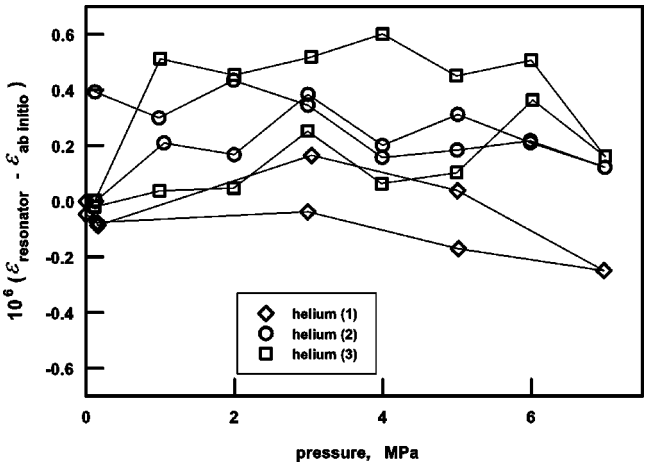

FIG. 7. Deviations of $\epsilon_r(p,T)$ values for helium determined with the resonator from *ab initio* values. The resonator values were calculated using Eq. (14) and a value of k_T taken from the literature (Ref. 14).

$$\epsilon_r(p,t) = \frac{C_x(p,T)}{C_x(0,T)}(1 + k_{T,invar}p/3), \tag{18}$$

where $k_{T,invar}$ is the isothermal compressibility of the superinvar alloy used to construct the cross capacitor, which was determined previously.[4] From each measurement, we formed the ratio

$$\Re = \frac{\epsilon_{r,capacitor}}{\epsilon_{r,resonator}}, \tag{19}$$

where $\epsilon_{r,resonator}$ was calculated from Eq. (14) and $\epsilon_{r,capacitor}$ was calculated from Eq. (18). The ratio $\Re$ is a measure of the consistency of the dielectric permittivity determined by two independent techniques with entirely different systematics, and is independent of gas pressure and composition. Figure 8 shows the variation of $\Re$ as the helium and argon pressures were varied at 288.94 K and the level of agreement is remarkably good. For helium, the values of $\epsilon_r(p,T)$ from the two instruments differed by 1×10^{-6} or less. For argon, there is a systematic trend in the value $\Re$ with pressure; however it is small with an average value of -1.4×10^{-6}. This is well within the capacitance bridge manufacturer's claimed uncertainty, and is possibly a measure of the bridge's degree of linearity. Furthermore, the argon results are consistent with the 1.0×10^{-6} difference that Schmidt and Moldover[5] found when comparing two cross capacitors in the same gases using a more accurate capacitance bridge.

Hysteresis was observed in the resonator values of $\epsilon_r(p,T)$ taken with increasing and decreasing pressures, and is apparent in both Figs. 7 and 8. For the three helium runs (Fig. 7), these data taken days apart reproduced themselves with standard deviations $\sigma=0.11\times10^{-6}$, 0.17×10^{-6}, and 0.16×10^{-6}. For the argon run, the values of $\epsilon_r(p,T)$ were less reproducible: $\sigma=0.43\times10^{-6}$ (Fig. 8, top). If the irreproducibility were caused by hysteresis in the deformation of the resonator with pressure, the helium and argon results would have been similar. For helium, we speculate that the reproducibility was limited by long-term "noise" in the temperature measurements. (Temperature drifts with $\sigma=5$ mK coupled to the thermal expansion of copper[14] (16.7×10^{-6} K^{-1}) cause $\sigma=0.17\times10^{-6}$ for $\epsilon_r(p,T)$ of either gas.) Since the pressure dependence of $\epsilon_r(p,T)$ is 8 times larger for argon than for helium, "noise" in the pressure measurements might contribute to the irreproducibility of the argon results. [Pressure drifts with $\sigma=70$ Pa would cause $\sigma=0.4\times10^{-6}$ for $\epsilon_r(p,T)$ of argon.] These speculations will be tested in future measurements.

VIII. DISCUSSION

We have demonstrated two significant results. First, that quasi-spherical cavity resonators could be used to measure the permittivity of the noble gases as accurately or more accurately than other well-documented techniques. Such cavities are promising candidates for dielectric constant gas thermometry and for realizing the proposed primary pressure standard based on the calculated permittivity of helium. Second, the theory of quasi-spherical cavities, when combined with accurate dimensional measurements, accurately predicts the frequency splittings of the microwave spectrum. This encourages further theoretical development to predict the dispersion of the microwave spectrum. If this is successful, the microwave spectrum could be used to accurately determine the volume of such a cavity.

To exploit the precision that quasi-spherical cavities offer, we require accurate values of the isothermal compressibility of the cavity. Thus, research on cavities must include accurate determinations of the elastic properties of the actual materials from which the cavity is constructed. We are using resonant ultrasound spectroscopy[25] to re-determine the elastic properties of the OFHC copper and other materials from which the cavities may be constructed.

ACKNOWLEDGMENTS

The authors thank John Stoup of the Precision Engineering Division at NIST for advice in planning the coordinate metrology and for operating the coordinate measurement machine. The authors thank Brian Dutterer and Blaine Young of the Fabrication Technology Division at NIST for fabricating

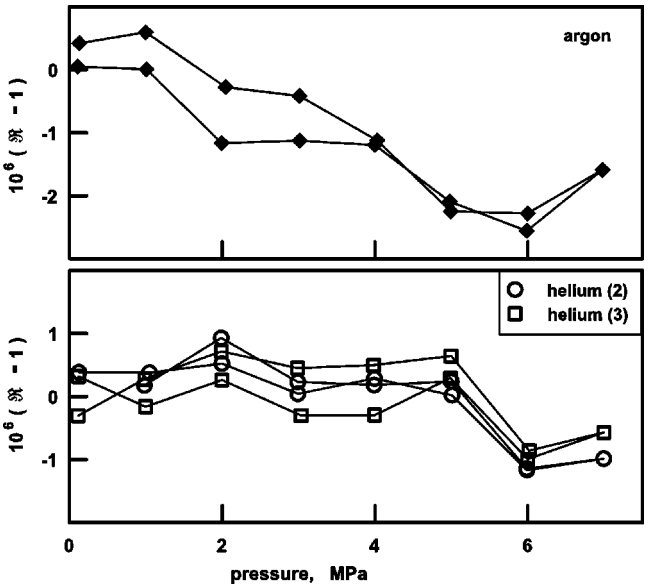

FIG. 8. Consistency of $\epsilon_r(p,T)$ values determined with the cavity resonator and the cross capacitor. The quantity $\mathfrak{R}$ is the ratio of $\epsilon_r(p,T)$ determined with the cross capacitor to the value determined simultaneously with the cavity resonator.

the resonators and for helpful discussions on the machining process. The authors are grateful to Yicheng Wang for the loan of the capacitance bridge. E.F.M. is supported in part by an AAA/ANZ Education Fellowship. The authors also thank Rich Davis, Ken Hill, and Rod White for carefully reviewing the manuscript.

[1] H. Luther, K. Grohmann, and B. Fellmuth, Metrologia **33**, 341 (1996).
[2] M. R. Moldover, J. Res. Natl. Inst. Stand. Technol. **103**, 167 (1998).
[3] G. Lach, B. Jeziorski, and K. Szalewicz, Phys. Rev. Lett. **92**, 233001 (2004).
[4] M. R. Moldover and T. J. Buckley, Int. J. Thermophys. **22**, 859 (2001).
[5] J. W. Schmidt and M. R. Moldover, Int. J. Thermophys. **24**, 375 (2003).
[6] J. A. Stone and A. Stejskal, Metrologia **41**, 189 (2004).
[7] M. B. Ewing and D. D. Royal, J. Chem. Thermodyn. **34**, 1985 (2002).
[8] B. Fellmuth, J. Fischer, C. Gaiser, and N. Haft, *Proceedings of TEMPMEKO 2004*, Dubrovnik, Croatia.
[9] M. E. Tobar, J. G. Hartnett, and J. D. Anstie, Phys. Lett. A **300**, 33 (2002).
[10] J. B. Mehl, M. R. Moldover and L. Pitre, Metrologia **41**, 295 (2004).
[11] R. F. Harrington, *Time-Harmonic Electromagnetic Fields* (McGraw-Hill, New York, 1961).
[12] L. W. Bruch and F. Weinhold, J. Chem. Phys. **113**, 8667 (2000).
[13] C. Barter, R. G. Meisenheimer, and D. P. Stevenson, J. Phys. Chem. **64**, 1312 (1960).
[14] N. J. Simon, E. S. Drexler, and R. P. Reed, *NIST Monograph 177: Properties of Copper and Copper Alloys at Cryogenic Temperatures* (U.S. Government Printing Office, Washington, 1992).
[15] J. D. Jackson, *Classical Electrodynamics*, 3rd ed. (Wiley, New York, 1999), p. 455.
[16] M. E. Tobar, J. D. Anstie, and J. G. Hartnett, IEEE Trans. Ultrason. Ferroelectr. Freq. Control **50**, 1407 (2003).
[17] J. Q. Shields, IEEE Trans. Instrum. Meas. **IM-27**, 464 (1978).
[18] J. Q. Shields, IEEE Trans. Instrum. Meas. **IM-21**, 365 (1972).
[19] L. R. Pendrill, J. Phys. B **29**, 3581 (1996).
[20] P. J. Leonard, At. Data Nucl. Data Tables **14**, 21 (1974).
[21] J. B. Mehl and M. R. Moldover, Phys. Rev. A **34**, 3341 (1986).
[22] M. E. Tobar, J. Phys. D **26**, 2022 (1993).
[23] M. R. Moldover, S. J. Boyes, C. W. Meyer, and A. R. H. Goodwin, J. Res. Natl. Inst. Stand. Technol. **104**, 11 (1999).
[24] J. B. Mehl, J. Acoust. Soc. Am. **79**, 278 (1986).
[25] A. Migliori and J. L. Sarrao, *Resonant Ultrasound Spectroscopy* (Wiley, New York, 1997).